Journal of Environmental Radioactivity 186 (2018) 152–160

Contents lists available at ScienceDirect

Journal of Environmental Radioactivity

journal homepage: www.elsevier.com/locate/jenvrad

Natural and artificial radionuclides in a marine core. First results of ^{236}U in North Atlantic Ocean sediments

M. Villa-Alfageme[a,*], E. Chamizo[b], F.J. Santos-Arévalo[b], J.M. López-Gutierrez[b,c], I. Gómez-Martínez[b], S. Hurtado-Bermúdez[d]

[a] Dpto. Física Aplicada II, Universidad de Sevilla, Av. Reina Mercedes 4A, 41012, Sevilla, Spain
[b] Centro Nacional de Aceleradores, Universidad de Sevilla, C Thomas Alva Edison, 7, 41092, Sevilla, Spain
[c] Dpto. Física Aplicada III, Universidad de Sevilla, Virgen de África, 41011, Sevilla, Spain
[d] Centro de Investigación, Tecnología e Innovación CITIUS, Universidad de Sevilla, Av. Reina Mercedes 4B, 41012, Sevilla, Spain

ARTICLE INFO

Keywords:
Sediment core
Nuclear fuel reprocessing plants
Inventory
^{236}U
^{129}I
$^{239+240}$Pu

ABSTRACT

There are very few data available of ^{236}U in marine sediment cores. In this study we present the results from the first oceanic depth profile of ^{236}U in a sediment core sampled in the North Atlantic Ocean, at the PAP site (4500 m depth, Porcupine Abyssal Plain (PAP) site, 49°0′ N, 16°30′ W). Additionally, the sediment core was radiologically characterized through the measurement of anthropogenic ^{137}Cs, ^{239}Pu, ^{240}Pu, ^{129}I and ^{14}C and natural ^{210}Pb, ^{40}K and ^{226}Ra.

The measured ^{236}U concentrations decrease from about $90{\cdot}10^{6}$ at g^{-1} at the seafloor down to $0.5{\cdot}10^{6}$ at g^{-1} at 6 cm depth. They are several orders of magnitude lower than the reported values for soils from the Northern Hemisphere solely influenced by global fallout (i.e. from $2700{\cdot}10^{6}$ to $7500{\cdot}10^{6}$ at g^{-1}). ^{236}U/^{238}U atom ratios measured are at least three orders of magnitude above the estimated level for the naturally occurring dissolved uranium. The obtained inventories are $1{\cdot}10^{12}$ at m^{-2} for ^{236}U, 80 Bq m^{-2} for ^{137}Cs, 45 Bq m^{-2} for $^{239+240}$Pu and $2.6{\cdot}10^{12}$ at m^{-2} for ^{129}I. Atomic ratios for ^{236}U/^{239}Pu, ^{137}Cs/^{236}U and ^{129}I/^{236}U, obtained from the inventories are 0.036, 0.11 and 2.5 respectively. Concentration profiles show mobilization probably due to bioturbation from the abundant detritivore holothurian species living at the PAP site sea-floor. The range of ^{236}U, ^{137}Cs, $^{239+240}$Pu and ^{129}I values, inventories and ratios of these anthropogenic radionuclides are more similar to the values due to fall-out than values from a contribution from the Nuclear Fuel Reprocessing Plants dispersed to the south-west of the North Atlantic Ocean. However, signs of an additional source are detected and might be associated to the nuclear wastes dumped on the Eastern North Atlantic Ocean.

1. Introduction

Uranium-236 is a long-lived radioisotope ($T_{1/2}$ = $2.35{\cdot}10^{7}$ yr) (Flynn et al., 1972) that decays by alpha emission to ^{232}Th and is an almost entirely anthropogenic isotope. It is produced in nuclear reactors through the capture of a thermal neutron by ^{235}U or ^{239}Pu (followed by alpha decay of ^{240}Pu), or in nuclear weapon tests from the ^{238}U(n, 3n)^{236}U reaction induced by fast neutrons. It is also naturally produced in inferior amounts by galactic cosmic ray induced secondary neutrons and by neutrons originating from (α, n) reactions in the natural terrestrial environment. These processes lead to natural ^{236}U/^{238}U atom ratios that range from 10^{-14} (i.e. estimated for typical rocks) to 10^{-9} (i.e. maximum value measured in uranium ores) (Steier et al., 2008). However, the amount of ^{236}U in the environment mainly has an anthropogenic origin, leading to isotopic ratios between 10^{-9} and 10^{-4} in the environment (Steier et al., 2008; Wendel et al., 2013; Winkler et al., 2012 and references therein).

A total amount of 35 kg of mobile ^{236}U coming from natural sources has been estimated (Christl et al., 2012; Steier et al., 2008 and references therein). On the other hand, (i) between 900 and 1400 kg of ^{236}U were released globally during the period of atmospheric nuclear weapons testing (Sakaguchi et al., 2009; Winkler et al., 2012), (ii) inventories of 95 ± 32 kg have been recently assessed for the liquid effluents coming from the nuclear fuel reprocessing plants (NFRP) in Britain (i.e. Sellafield and Springfields), and in France (i.e. La Hague) (Christl et al., 2015), and (iii) about 100 kg of ^{236}U were dispersed over eastern Europe as a consequence of the Chernobyl accident (Castrillejo et al., 2017). The Sellafield and La Hague effluents dominate the concentrations of ^{236}U in the North Atlantic and Arctic Oceans (Casacuberta et al., 2014, 2016).

* Corresponding author.
E-mail address: mvilla@us.es (M. Villa-Alfageme).

http://dx.doi.org/10.1016/j.jenvrad.2017.10.001
Received 1 June 2017; Received in revised form 3 October 2017; Accepted 3 October 2017
Available online 20 October 2017
0265-931X/

Up to now, due to the difficulties in the measurement of low $^{236}U/^{238}U$ ratios, the availability of ^{236}U measurements in the environment was limited. After the improvement of the analytical detection techniques, AMS (Marsden et al., 2001), ICP-MS (Ketterer et al., 2003) or TIMS (Richter et al., 2010), ^{236}U concentrations data in several environmental compartments have become available in recent years. Furthermore, recent studies demonstrate the potential use of ^{236}U as an oceanic circulation (Christl et al., 2013; Sakaguchi et al., 2012), coral (Nomura et al., 2017; Winkler et al., 2012) and ice core (Wendel et al., 2013) tracer.

However, the biogeochemical characteristics of anthropogenic ^{236}U in seawater and particles are still not well constrained (Sakaguchi et al., 2012), e.g. its main oxidation state in the ocean is undetermined and also how this affects effectively to its scavenging by particles. Furthermore, preliminary results point out to a possible speciation between the dissolved and the particulate phases in seawater, which favours the ^{236}U concentration in the sediment (Eigl et al., 2017; Sakaguchi et al., 2012). Finally, it is necessary to better constrain the anthropogenic ^{236}U released, especially from the NFRP, and more particularly of Sellafield, and its pathways through the Atlantic and Arctic oceans. Recently, it has been modelled ^{236}U inputs from the NFRP, but further studies will be needed in order to increase the accuracy of the estimations (Christl et al., 2015). This is of primary importance in order to use $^{236}U/^{238}U$, and also $^{129}I/^{236}U$, as a sensitive tool for the calculation of tracer ages and ventilation rates in the North Atlantic domain (Casacuberta et al., 2016).

Pu as opposed to U is considered almost exclusively anthropogenic. Plutonium has a very different geochemical behaviour than uranium, it is complex because different valences plutonium isotopes coexist and constitute inorganic and organic ligands. In seawater it is a particle-reactive element that is exported in the water column with the sinking particles, and is re-mineralized in deep waters or stored in the sea-bed sediment (Chamizo et al., 2015). ^{210}Pb is a particle reactive tracer of natural origin widely used for core dating purposes (San Miguel et al., 2003) and evaluation of particle export fluxes (Le Moigne et al., 2013).

^{137}Cs and ^{129}I behave in seawater as a conservative tracer, with its distribution governed by physical transport ocean currents processes (Periáñez et al., 2016; Villa-Alfageme et al., 2015). Natural uranium is conservative in water (Owens et al., 2011) and the same behaviour has been predicted for ^{236}U (Casacuberta et al., 2014). However, ^{236}U adsorption properties in marine sinking particles and its mobility in the sediments is not well constrained. The four anthropogenic radionuclides have a contribution in seawater from fallout and they have been regularly released from NFRPs such as Sellafield and la Hague (Chamizo et al., 2015; Periáñez et al., 2016; Villa-Alfageme et al., 2015).

Therefore, there are several challenges that still must be solved when using anthropogenic ^{236}U as a tracer: i) to define its biogeochemical behaviour, ii) furthermore, it is necessary to better constrain the anthropogenic ^{236}U sources and specially quantify the NFRP annual releases and its pathways through the Atlantic and Arctic oceans. We investigated these topics, through the analysis of a marine sediment core collected in the North Atlantic at the Porcupine Abyssal Plain (PAP) site.

The analysis of a combined set of radionuclides with different sources (i.e. anthropogenic and naturally occurring) and with different behaviours in seawater (i.e.particle reactive, and conservative) is crucial to investigate on the biochemistry of anthropopgenic ^{236}U.

A full analysis of the artificial and natural radionuclides concentrations in the core was carried out additionally to ^{236}U. ^{129}I ($T_{1/2} = 1.57 \times 10^7$ yr) (Raisbeck and Yiou, 1999), ^{239}Pu ($T_{1/2} = 2.41 \times 10^4$ yr) (Prindle et al., 1978), ^{240}Pu ($T_{1/2} = 6.5 \times 10^3$ yr) (Ahmad et al., 2007), ^{14}C ($T_{1/2} = 5.73 \times 10^3$ yr) (Pettitt et al., 2003) were measured through AMS and ^{137}Cs ($T_{1/2} = 30.17$ yr) (Juget et al., 2016), ^{40}K ($T_{1/2} = 1.248 \times 10^9$ yr) (Mougeot, 2017), ^{210}Pb ($T_{1/2} = 22.3$ yr) (Villa et al., 2003)and ^{226}Ra ($T_{1/2} = 1.6 \times 10^3$ yr) (Villa et al., 2005) were measured by gamma spectrometry.

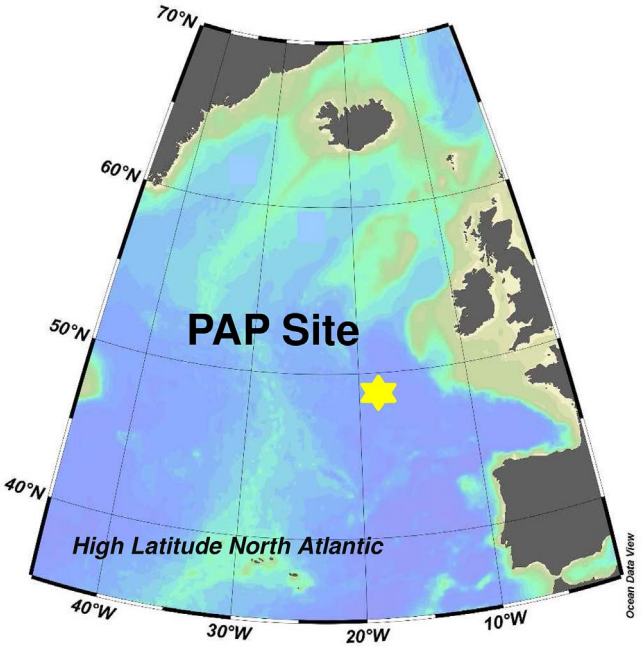

Fig. 1. Map of the sampling site. Porcupine Abyssal plain (PAP) site. Located in the North Atlantic Ocean.

Our results combine a very broad dataset of radionuclides that will be used to i) provide radioecological information of artificial and natural radionuclides in a North Atlantic sediment i) provide a first approach to the transport pathways and biogeochemical behaviour of ^{236}U in the environment and iii) analyse the different sources of ^{236}U to this marine sediment.

2. Sampling and methods

2.1. Sample collection and site description

The sediment core was collected at the PAP site (Fig. 1), at 48° 48.2′N and 16° 27.3′W and 4934 m depth, during the cruise D341 onboard R.R.S *Discovery* in July 2009 (Le Moigne et al., 2013). The samples were obtained using a multicorer and were sectioned into 0.5- or 1-cm intervals. Samples were stored frozen and returned to the shore-based laboratory for subsequent analysis. The Porcupine Abyssal Plain (49° N and 16° 30′ W), PAP site, is located on the boundary between the subpolar and subtropical gyres of the North Atlantic (Villa-Alfageme et al., 2014), adjacent to the Irish continental margin.

Porcupine Abyssal Plain megabenthos includes a large number of marine invertebrates. These animals are increasing in number as more phytodetritus falls to the seabed (Kalogeropoulou et al., 2010). Since 1996, an important change has taken place in the numbers of creatures living over a large area of the North Eastern Atlantic sea floor. Sea anemones, brittle stars, polychaete worms, sea spiders and particularly sea cucumbers on the deep sea floor have all increased significantly in numbers (Billett et al., 2001).

2.2. Actinides measurement

2.2.1. Reagents

For ^{236}U AMS determinations, it is very important to minimize the ^{238}U and ^{236}U contaminations introduced by reagents, spikes and laboratory materials. Therefore, the reagents used during the sample preparation were of the highest purity grade and glassware was avoided when possible. To prepare the AMS cathodes, an ultra-pure iron solution supplied by High Purity Standards (HPS, England) was used.

TEVA® and UTEVA® cartridges in a vacuum box, supplied by Eichrom Technologies LLC (France), were used for the final U and Pu purifications.

The ^{242}Pu and ^{233}U spikes, necessary to control the corresponding chemical recoveries, were obtained from the certified reference material R15-20 supplied by National Physical Laboratories (NPL, United Kingdom), and the certified reference material IRMM-058 supplied by the International Atomic Energy Agency Radiometrics Laboratory in Monaco (IAEA-MEL), respectively.

Before being used for this work, the presence of the isotopes of interest in these solutions was studied by AMS. Significant traces of ^{236}U were found in the case of the ^{233}U spike, with an atomic abundance of 10^{-3}. This background was substracted from the final ^{236}U/^{233}U AMS ratios.

2.2.2. Actinides measurement

Different sediment aliquots, ranging from 3 to 5 g each, were used for the ^{239,240}Pu and ^{236}U determinations. About 1 pg of the corresponding tracers were added to each aliquot. Given the nature and potential sources of anthropogenic radioactivity at the studied site, the samples were not expected to contain Pu isotopes and ^{236}U in refractory forms. Therefore, a simple leaching procedure, based on the addition of HNO_3 and H_2O_2 in a hot plate at atmospheric pressure, was applied to put in solution the Pu or U, following the guidelines given in Sakaguchi et al. (2009). Pu or U isotopes were purified using TEVA® or UTEVA® resins, according to their general elution behaviours reported by Eichrom. The sputter targets for the AMS measurements were prepared in an iron oxide matrix by a preliminar coprecipitation with $Fe(OH)_3$ and a final oxidation at 800 °C for 2 h. Non-reusable quartz crucibles were used in this final stage to avoid contamination. Details about the chemical procedures can be found in (Chamizo et al., 2008, 2015).

AMS determinations were carried out on the 1 MV CNA AMS facility in 2013 using Ar gas as stripper. The Pu AMS measurement technique is described in Chamizo et al. (2008). Details about the ^{236}U AMS measurement technique are given in (Chamizo et al., 2015). Briefly, actinides (Ac) are extracted from the Cs-sputter ion source as $Ac^{16}O^-$ at 35 keV, stripped to Ac^{3+} in Ar gas stripper at 670 kV terminal voltage with about 11% yield, and finally counted from the total energy signal provided by a gas ionization chamber. The different isotopes of interest (^{239,240,242}Pu for Pu analysis and ^{233,236,238}U for ^{236}U studies) were measured sequentially using the so-called *Slow Sequential Injection System*.

The necessary homogeneity test for the studied samples was performed by analysing the ^{239,240}Pu concentration in two different aliquots of three different samples. Results from Table 1 show that the reproducibility of the results is excellent.

The whole methodology (sample preparation and measurement technique) was successfully validated through the measurement of a set of reference materials affected by different actinide sources supplied by the IAEA: IAEA-Soil-6, surface soil from Austria solely influenced by global fallout; IAEA-375, soil collected from a farm close to Chernobyl; IAEA-385, sediment from the Irish Sea; IAEA-384, from the former French nuclear test site at Mururoa and Fangataufa; and the IAEA-RGU uranium mineral (Chamizo et al., 2015). Background values of about 10^6 atoms have been obtained for plutonium isotopes, as explained in (Chamizo et al., 2008). As for ^{236}U, abundance sensitivity for the ^{236}U/^{238}U ratio of 5×10^{-11} has been estimated (Chamizo et al., 2015).

Table 1
$^{239+24}$0Pu activity concentration obtained in two different aliquots of three different samples from PAP site sediment.

Sample	M (g)	$^{239+240}$Pu (mBq g^{-1})	± 1σ
PAP-0-0.5	3,41	0,293	0006
	0,62	0,310	0010
PAP-1-1.5	5	0,312	0010
	3,01	0,340	0006
PAP-2-2.5	5,03	0,192	0004
	2,35	0,182	0004

2.3. ^{14}C measurement

2.3.1. Sample preparation

Both organic and inorganic carbon fractions were prepared from the sediment to be radiocarbon dated. In both cases, the main idea is to convert the carbon into CO_2, and then reduce it to graphite in the so called graphitization process.

For the inorganic fraction, CO_2 was obtained through acid leaching with phosphoric acid under vacuum conditions. CO_2 was transferred to a manual graphitization line based on (Hajdas et al., 2004). There CO_2 was reduced to graphite by the addition of H2, using cobalt as a catalyst, at 625 °C. Standard and blank samples used to normalize and background correction in these samples were prepared in the same graphitization line. Oxalic Acid II from NIST (Mann, 1983) was used as the standard, and C1 material from IAEA was used as a blank (Rozanski et al., 1992).

For the organic fraction, the carbonate was eliminated by acid leaching with HCl 0.5 M, in order to get a higher concentration of organic carbon in the sediment. Total organic fraction was graphitized using a combined system of an elemental analyzer and an AGE system (Wacker et al., 2010c). The elemental analyzer combusts the sample to CO_2 and this is automatically transferred to the AGE system to be reduced to graphite. As with the inorganic fraction, standard and blank samples were prepared also in AGE to ensure the maximum similarities. Fossil wood was used as a blank in this case.

In both cases the objective is to get approximately 1 mg of carbon for the AMS measurement. The graphite, mixed with the catalyst, is pressed in the target and is ready to be measured.

2.3.2. AMS measurement

^{14}C measurements were performed at a Micadas system (Wacker et al., 2010a) at CNA. Micadas is an AMS system optimized for radiocarbon detection at very low energies, using a terminal voltage of 200 kV. It follows the sample principles of operation as other AMS systems. Samples are sputtered in the ion source and C- ions are extracted as a beam. After a first magnetic selector, ions are accelerated and the stripping process changes the state of charge of the ions. 1 + ions are selected to further filtration in the high energy side, and are finally detected in a gas ionization counter. Stable isotopes are measured in the high energy side by several Faraday cups.

Each sample is measured for about 60 min in several cycles to ensure the stability of the measurement. Data analysis is performed with the software BATS(Wacker et al., 2010b), obtaining the final results. Results are reported as advised in Stuiver and Polach (1977), corrected by fractionation (Stuiver and Polach, 1977).

In order to validate our procedures, covering the whole sample preparation and measurement, our laboratory participated in the Sixth International Radiocarbon Intercomparison (SIRI) that provided the latest set of samples for laboratories to check their AMS facilities for ^{14}C dating A set of SIRI samples including a total of thirteen samples (seven wood samples, two bone samples, and one each of barley mash, charcoal, carbonate and humic acid), and additionally C7 and C8 IAEA reference samples, were prepared following routine procedures used in our lab. Finally, a general good agreement in the results was achieved (Santos-Arévalo et al., 2015). The achieved blank levels for the so-called IAEA-C1, Carrara marble, and for the carbonate sample Doublespar from Iceland, kindly provided by Prof. J. Heinemeier, range from 0.002 to 0.004 F^{14}C (F stands for fraction of modern carbon), which is equivalent to approximately 50,000–45,000 years BP or a^{14}C/^{12}C ratio of $\sim 3 \times 10^{-15}$ (Calvo et al., 2015).

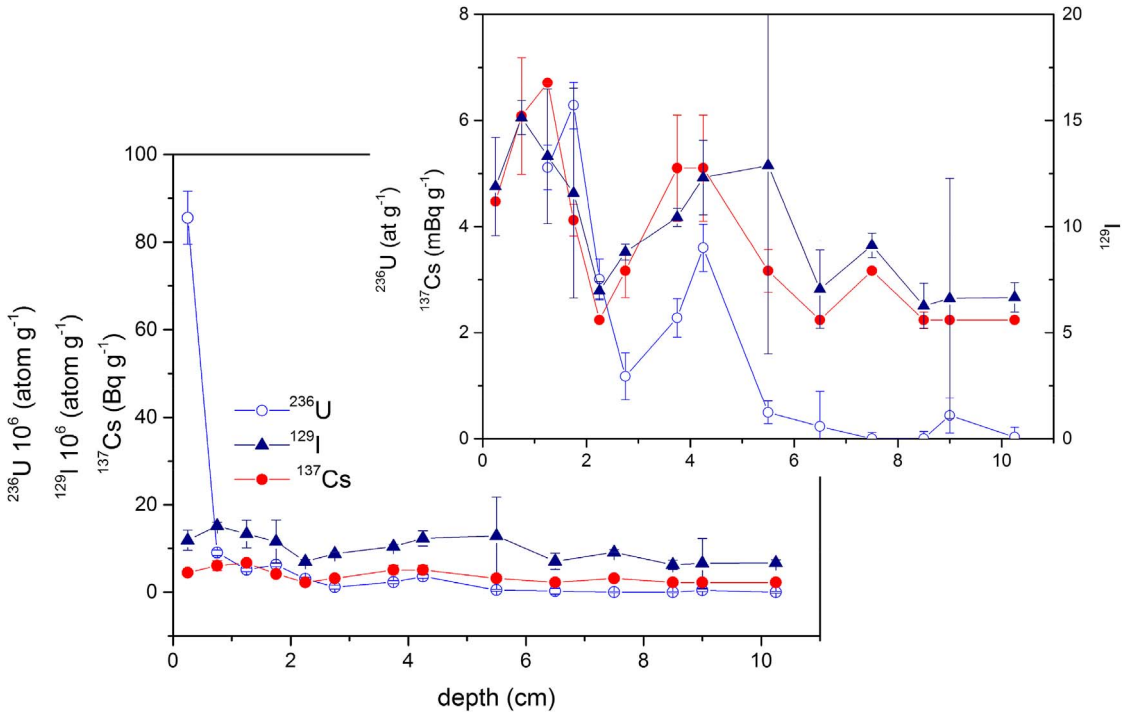

Fig. 2. ^{236}U (at g^{-1}), ^{129}I (at g^{-1}), ^{137}Cs (mBq g^{-1}) concentrations at the PAP site sediment core, from surface to 10.25 cm depth. Uncertainties correspond to 1 sigma.

2.4. ^{129}I measurement

2.4.1. Sample preparation

In order to obtain the ^{129}I concentration in the samples, a carrier-addition method applied. A total of 3 mg iodine carrier (Woodward Inc. Iodine) were added to 2 mg sediment. Then, the isotopic ratio measured by Accelerator Mass Spectrometry (AMS) is approximately the ratio between ^{129}I from the sediment and stable iodine from the carrier. Solid NaOH (6 g, Panreac, PA-ACS-ISO) is added to the mixture in a nickel crucible and heated in an oven for 1 h at 150 °C, then for 2 h at 200 °C followed by 3 h at 275 °C. The melt is extracted, centrifuged and all species are then reduced to iodide by the addition of 0.1 M NaHSO3 (prepared from $Na_2S_2O_5$, Panreac PA-ACS) to the supernatant. After that, in order to oxidise iodide, $NaNO_2$ (Panreac PA-ACS) is added and the solution is acidified with 6 HNO_3 (Panreac 65% PA-ISO). Iodine is then extracted into chloroform (Panreac) in a separating funnel and back-extracted into aqueous $NaHSO_3$ solution. These purification steps are repeated twice. Saturated $Ba(NO_3)_2$ (from Panreac PRS) is then added in order to precipitated exceeding SO_3- as $BaSO_3$ and avoid precipitation of Ag_2SO_3 afterwards. Finally, AgI is precipitated by the addition of $AgNO_3$ (Merck, ACS reagent, ≥99.0%) mixed with Nb powder (< 45 μm, 99.8%, Sigma-Aldrich) and pressed into a Cu cathode for AMS measurement. More details can be found in (Szidat et al., 2000).

2.4.2. AMS measurement

^{129}I AMS measurement are described (Gómez-Guzmán et al., 2012). Measurements were carried out at the 1 MV AMS facility at the Centro Nacional de Aceleradores in Sevilla (CNA, Spain). Iodine is extracted as I- from a Cs sputtering ion source at 26 keV. Characteristic currents at the low energy side are between 1 and 5 μA. After a first magnetic deflector, ions are injected into the tandem accelerator. The terminal voltage is 1 MV and the selected charge state is 3+, for which transmission is approximately 9%. $^{129}I^{3+}$ ions are detected in a gas ionization chamber after a magnetic and an electrostatic deflector, while $^{127}I^{3+}$ ions are measured as a current in a Faraday cup. Machine background values are typically $^{129}I/^{127}I \cong 3 \times 10^{-13}$, which is typically one order of magnitude under the isotopic ratios measured for real samples. Chemical blanks were prepared routinely every four or five samples and showed results slightly higher than the instrumental blank.

AMS measurements are performed relative to standards with known $^{129}I/^{127}I$ ratios. The used ^{129}I standards were made by repeated dilutions from NIST SRM 3230 Iodine Isotopic Standard Level I, with a certified $^{129}I/^{127}I$ ratio of $(4.920 \pm 0.062) \times 10^{-10}$. Calibration standards with $^{129}I/^{127}I$ ratios of about 10^{-10}, 10^{-11}, 10^{-12} and 10^{-13} were measured obtaining an agreement between all of the measured calibration standards and their nominal values in a wide dynamic range (Gómez-Guzmán et al., 2012).

2.5. Gamma spectrometry

Total ^{210}Pb activity was determined by its gamma emission at 46.5 keV, ^{226}Ra activity was estimated from the 295 and 352 keV γ-rays emitted by its daughter isotope ^{214}Pb. For ^{228}Ra gamma emission from ^{228}Ac (338.4, 911.1 and 583 keV) was used. ^{40}K was estimated through 1460.8 keV emission. ^{137}Cs was measured by its emission at 662 keV. The absolute efficiencies of the detectors were determined using calibrated sources, and corrections were made for the effect of self-absorption of low energy gamma-rays within the sample.

Each sample was counted for 1–3 days, and activity values were standardised using IAEA reference materials (IAEA-444 and IAEA-447). The specific activity (in Becquerels per kilogram) of each sediment sample was calculated from the detector efficiency, gamma intensity and sample weight. All values are reported as the activity on the date of sampling. Uncertainties reflect one sigma counting statistics. The main gamma-ray detector was a low-background Canberra high-purity germanium (HPGe) GCW-3023-S well-type coaxial detector surrounded by a 10 cm thick, high-purity lead shield and antiCompton NaI(Tl) annular crystal.

The validation of the gamma-ray spectrometry methodology was based on the successful participation on several intercomparison exercises promoted by ICRM working group related to efficiency calibration and coincidence-summing correction (Lépy et al., 2012)

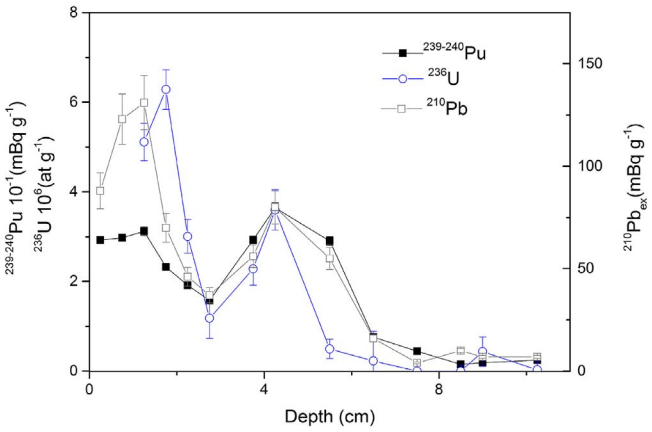

Fig. 3. ^{236}U (at g^{-1}), $^{239-240}$Pu (mBq g^{-1}), ^{210}Po (mBq g^{-1}) concentrations at the PAP site sediment core, from surface to 10.25 cm depth. In the case of ^{236}U, the surface maximum is not represented. Uncertainties correspond to 1 sigma.

(Vidmar et al., 2008), together with the strongly measurement of IAEA certified materials (Mantero et al., 2015) or the comparable results against those obtained with other techniques as alpha-particle spectrometry (Jiménez-Ramos et al., 2010). It was also determined the Minimum Detectable Activity (MDA) of system ^{40}K, ^{137}Cs, ^{210}Pb, ^{226}Ra, obtaining respectively 20 mBq/kg, 0.1 mBq/kg, 11 mBq/kg, and 9 mBq/kg (Hurtado et al., 2006).

3. Results and discussion

3.1. Concentration depth profiles

Fig. 2 shows the depth profiles in the sediment core from 0 to 10.5 cm for the radionuclides considered conservative in seawater: ^{129}I, ^{137}Cs and ^{236}U. Fig. 3 presents the particle reactive ^{210}Pb and ^{239}Pu, together with ^{236}U from 0.75 cm depth (i.e. without the surface maximum), for comparison. All the results are displayed in Table 3.

Specific activities of naturally occurring radionuclides ^{40}K, ^{210}Pb and ^{226}Ra in the core samples are shown in Table 2. The measured values are quite similar to those of typical marine sediments (Laissaoui et al., 2013; San Miguel et al., 2003; Villa et al., 2009). ^{226}Ra activity was fairly constant along the core, this is expected, since the deposition of ^{226}Ra from particle scavenging or redisolution from water is negligible and we are measuring the concentrations of ^{226}Ra naturally present in the sediment (see Table 2).

Table 2
^{210}Po, ^{226}Ra, ^{40}K concentrations at the PAP site sediment. Uncertainties correspond to 1 sigma.

Sample	Depth (cm)	^{210}Pb (mBq g^{-1})	± σ	^{226}Ra (mBq g^{-1})	± σ	^{40}K (mBq g^{-1})	± σ
PAP-0-0.5	0.25	103	4	16	2	70	9
PAP-0.5-1	0.75	133	20	18	3	90	10
PAP-1-1.5	1.25	160	10	17	1	71	8
PAP-1.5-2	1.75	83	3	18	2	91	8
PAP-2-2.5	2.25	73	5	19	3	90	15
PAP-2.5-3	2.75	61	2	19	1	98	7
PAP-3.5-4	3.75	90	10	17	1	95	9
PAP-4-5	4.25	100	6	20	1	91	7
PAP-5-6	5.5	98	5	19	1	94	6
PAP-6-7	6.5	50	4	20	1	90	10
PAP-7-8	7.5	45	10	20	1	140	10
PAP-8-9	8.5	42	4	21	1	140	10
PAP-9-10	9	44	2	21	2	210	10
PAP-10-10.5	10.25	47	1	21	1	212	8

On the contrary, there is an atmospheric deposition of ^{210}Pb in the surface ocean and a subsequent scavenging and deposition in the seafloor by the sinking particles. There is also a contribution of ^{210}Pb from the ^{226}Ra decay in the sediment, therefore, it is usually calculated what is called ^{210}Pb excess (^{210}Pb$_{ex}$), that correspond to the ^{210}Pb concentrations excluding the contribution from ^{226}Ra. An exponential decay in depth is the simplest profile that describes ^{210}Pb$_{ex}$ (San Miguel et al., 2004) for soils or sediment profiles where the sedimentation rates are significant (i.e. at the cm y^{-1} level). However the data displayed in Fig. 2 corresponds to two maximums, one near the surface and a second one at 4–5 cm that are very unlikely to be produced by atmospheric deposition and subsequent mixing processes, given the extremely low sedimentation rates that are expected in abyssal sediments (i.e 0.0014–0.032 mm y^{-1}). A very similar shape is found for $^{239+240}$Pu. Fig. 2 shows similar patterns for the conservative radionuclides.

The ^{14}C profiles in the organic and the carbonate fractions differs considerably (Fig. 4), and the two maxima are only seen in the organic fraction. On the contrary, the ^{14}C fraction in the carbonates remains constant in the first 6 cm depth. Pointing out that the organic phase corresponds to a recent deposition of the sinking particles, in contrast to the carbonates fraction.

Note that PAP site deep sea-floor is a biogenous sediment with a deposition rate of 0.0014–0.032 mm y^{-1} (Carvalho et al., 2011). That implies that most of the anthropogenic radioactivity due to fallout and particles deposition should be located in the very first two centimetres of the sediment. Figs. 1 and 2 shows that not only ^{137}Cs, ^{236}U and ^{129}I are mobile in this core, but also refractory radionuclides such as ^{210}Pb and $^{239+240}$Pu. One of the possible explanations for this behaviour is that the sediment has been completely perturbed due to bioturbation (Stordal et al., 1985). The same effect was observed in the past over the North Atlantic Ocean for $^{239+240}$Pu and ^{210}Pbex sediment depth profiles (Buesseler and Sholkovitz, 1987).

Since 1995–1996, the number of creatures living over a large area of the North Eastern Atlantic sea floor increased considerably, e.g. sea anemones, brittle stars, polychaete worms, sea spiders and particularly sea cucumbers (Billett et al., 2001). The number of the large invertebrates increased by at least a hundredfold. One sea cucumber species, *Amperima rosea*, increased its number from 2 to 3 individuals per hectare to more than 6000 (Billett et al., 2010). These species work over the sediment on the sea floor, where they feed, and the sediment is quickly processed. It used to take the animals two and a half years to reprocess the sediment, but after 1996 it took less than 6 weeks (Bett et al., 2001). These creatures feed at the surface of sediment by filtering them and the two different maxima might correspond to the depths where they excrete.

Mobile radionuclides (^{129}I and ^{137}Cs) penetrates even deeper in the core (below 10 cm), whereas $^{239+240}$Pu and ^{210}Pb remains mainly in the first 7 cm.

Uranium in seawater is usually oxidized to hexavalent uranium, which is highly soluble as the uranyl ion UO_2^{2+} × U(VI) is the major form of U in oxic surface (Cumberland et al., 2016) waters, hence ^{236}U is considered a conservative radionuclide in seawater, as ^{129}I or ^{137}Cs. However, note that U(IV) would be the major form in anoxic waters (Maher et al., 2012). However, in the sediment analysed ^{236}U behaviour differs from the one of ^{129}I and ^{137}Cs. First, most part of the ^{236}U is accumulated on the surface of the sea-bed sediment, 80·10^6 at g^{-1} in surface versus 10·10^6 at g^{-1} and exclusively ^{236}U present this pattern, this increase might be due to an additional source of ^{236}U in the sediments that will be later described. When the results for ^{236}U are zoomed in for deeper depths and compared with the profiles of conservative (Fig. 2) and particle reactive (Fig. 3) radionuclides, we find out that in this sediment the behaviour of uranium is more similar to the particle reactive radionuclides profiles.

The speciation of uranium (U) in water might undergo several changes in the presence of the ligands commonly found in natural waters also in the sediment U(VI) is reduced to U(IV) in the anoxic

Table 3
^{236}U, ^{239}Pu, ^{129}I, ^{14}C (in carbonates and in the organic fraction) and 137Cs concentrations at the PAP site sediment. Uncertainties correspond to 1 sigma.

Sample	Depth (cm)	^{236}U (10^6 at g^{-1})		^{239}Pu (10^6 at g^{-1})		^{14}C carbonates (pMC)		^{14}C organic (pMC)		^{137}Cs (mBq g^{-1})	
PAP-0-0.5	0.25	86	6	208	4	71.2	0.3	85.2	0.4		
PAP-0.5-1	0.75	9.0	0.7	208	5	69.6	0.3	60.7	0.3	1.10	0.20
PAP-1-1.5	1.25	5.1	0.4	221	7	68.9	0.4	58.5	0.3		
PAP-1.5-2	1.75	6.3	0.4	168	3	68.6	0.3	54.9	0.3	0.30	0.08
PAP-2-2.5	2.25	3.0	0.4	133	3	69.8	0.3	78.3	0.3		
PAP-2.5-3	2.75	1.2	0.4	113	5	67.1	0.3	53.9	0.3	0.50	0.10
PAP-3.5-4	3.75	2.3	0.4	215	6	68.5	0.4	48.0	0.3	1.00	0.20
PAP-4-5	4.25	3.6	0.4	265	8	68.7	0.3	56.2	0.3	1.00	0.20
PAP-5-6	5.5	0.5	0.2	194	6	68.4	0.3	61.7	0.3	0.40	0.10
PAP-6-7	6.5	0.2	0.7	48	3	63.6	0.3	46.9	0.2		
PAP-7-8	7.5	0.00026	0.12	30	1	57.6	0.3	49.9	0.3		
PAP-8-9	8.5	0.00026	0.13	11	2	49.4	0.3	43.9	0.2	0.15	0.07
PAP-9-10	9	0.4	0.3	12	1	39.1	0.2	38.2	0.2		
PAP-10-10.5	10.25	0.0	0.2	17	1	37.0	0.2	31.8	0.2		

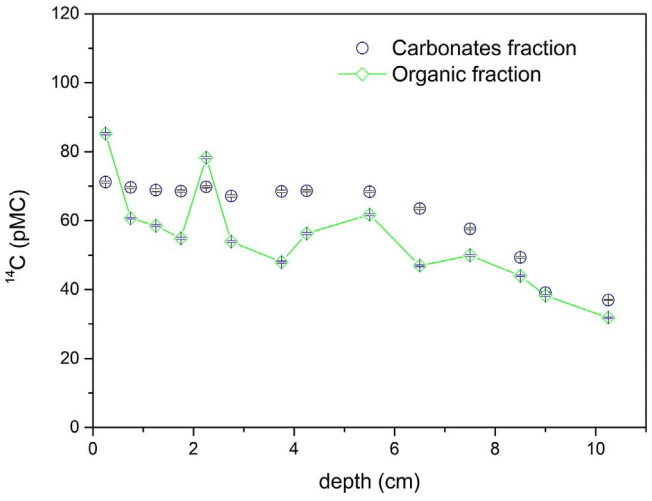

Fig. 4. ^{14}C (pMC) concentrations at the PAP site sediment core, from surface to 10.25 cm depth in the carbonates and organic fractions. Uncertainties correspond to 1 sigma.

sediment (Maher et al., 2012) and this is probably happening at the PAP site bed-sediment, since U(IV) minerals are highly insoluble and immobile (Morris and Raiswell, 2002). This is the reason why most of the ^{236}U is found in the depths affected by bioturbation but, just like $^{239+240}Pu$, do not reach the deepest layers, down to 10.5 cm, as ^{137}Cs and ^{129}I do.

The significant increasing of ^{236}U in the first layer and the fact that this increasing is specially significant for ^{236}U, and in comparison with the other radionuclides, suggests the existence of a specific source of ^{236}U in the area, additional to fall-out. It is usually assumed that most of the liquid discharges carrying the radionuclides from the NFRP enters into the Norwegian Coastal Current (Christl et al., 2015); however, some evidences are found that part of the releases might be distributed South-Eastern into the North Atlantic Ocean (Gomez-Guzman et al., 2013; Villa-Alfageme et al., 2015). Nevertheless, according to the concentration data provided by Villa-Alfageme et al. (2015), it is unlikely that the increase measured in our core corresponds to ^{236}U releases from the NRFP. The cause of this increase is examined in the next sections, including inventories and the evaluation of the complete dataset of radionuclides.

3.2. Isotopic ratios and inventories

Table 4 presents different isotopic ratios for the measured anthropogenic radionuclides and in Table 5 are shown their inventories in the sediment core and $^{236}U/^{239}Pu$ and $^{137}Cs/^{236}U$ ratios calculated from these inventories. Inventories were calculated using a straightforward rectangle method to integrate the radionuclides concentration.

$^{239}Pu/^{240}Pu$ ratios are fairly constant in depth, 0.155 ± 0.019 atom ratios, the values are slightly lower than the reported one for the general fallout in the Northern Hemisphere (i.e. de 0.178 ± 0.019 for the 0-30° northern latitude (Kelley et al., 1999)), and far from the atom ratio in marine sediment reference sample, IAEA-135, collected close to the NFRP, 0.21 at at^{-1} (Chamizo et al., 2015). Thus, according to $^{239}Pu/^{240}Pu$ ratios, no plutonium contribution from the NFRP is detected in the core from the PAP site. This would be expected since plutonium is a very particle reactive radionuclide, and even if assuming that part of the releases from the NFRP are headed southwards, plutonium would be fast scavenged from the surface by the sinking particles and by remobilization of the sediments of the continental platform before it reaches PAP site.

$^{236}U/^{239}Pu$ atom ratio is 0.41 ± 0.03 at surface, but drops to values at the 0.03–0.01 interval for most of the samples, this is in agreement with the expected ratios for marine sediments impacted by global fallout or NFRP (i.e. of about 0.1–0.02 (Chamizo et al., 2015)). This confirms a higher mobility of ^{236}U in relation to plutonium. The total ratio $^{236}U/^{239}Pu$ provided by the inventories, 0.0357, is clearly lower than the ratio measured in IAEA-135, Irish Sea, 0.1, but higher of the ratio measured in the reference samples IAEA-412 at the Pacific Ocean, exclusively affected by fallout, with a ratio of about 0.02 (Chamizo et al., 2015).

On the other hand, $^{129}I/^{236}U$ increases with depth, suggesting a significantly higher mobility of ^{129}I within the sediment. The analysis of the ratio $^{137}Cs/^{236}U$ confirms a different behaviour of ^{236}U in relation to conservative ^{129}I and ^{137}Cs in the sediment, since these ratios also increases with depth. When we compare the isotopic ratio from PAP site, $8\ 10^{-11}$, to the one measured in the Japan Sea (39°32.56′N), $2.4\ 10^{-10}$ (Sakaguchi et al., 2012), we detect a higher contribution of ^{236}U at PAP site than in the Japan Sea, in relation to ^{137}Cs inventories. A similar contribution for both radionuclides from global fallout would be expected at both sites, as they are located at similar northern latitudes (49°N and 39°N, respectively). This result suggests the existence of an additional source of ^{236}U in the area.

To explore the existence of an additional source in the area in relation to other radionuclides we compare the inventories of $^{239+240}Pu$ and ^{137}Cs (see Fig. 5 and Table 5) and the ratios $^{137}Cs/^{129}I$ and $^{239+240}Pu/^{137}Cs$ in different marine sediments (see Fig. 6 and Tables 4 and 5).

^{137}Cs inventories, though slightly higher than in other areas (Fig. 5 and Table 5), do no differ significantly at the PAP site and at the Mediterranean Sea, being this last one more influenced by the Chernobyl accident. On the contrary $^{239+240}Pu$ inventories at PAP site are twice higher than the ones at Bermuda and the Mediterranean Sea.

The ratios $^{137}Cs/^{129}I$ are very variable within the Irish sea, affected by direct releases from Sellafield. The isotopic ratio at the PAP site is

Table 4
Atom ratios $^{239}Pu/^{240}Pu$, $^{236}U/^{239}Pu$, $^{137}Cs/^{236}U$ and $^{129}I/^{236}U$ measured at the PAP site sea-bed sediment core, from surface to 10.25 cm depth. Uncertainties correspond to 1 sigma.

Sample	Depth (cm)	$^{239}Pu/^{240}Pu$ (at at^{-1})		$^{236}U/^{239-240}Pu$ (at at^{-1})		$^{137}Cs/^{236}U$ (at at^{-1})		$^{129}I/^{236}U$ (at at^{-1})		$^{137}Cs/^{129}I$ (at at^{-1})	
PAP-0-0.5	0.25	0.145	0.007	0.41	0.03			0.14	0.03		
PAP-0.5-1	0.75	0.154	0.008			0.17	0.03	1.7	0.2	0.10	0.03
PAP-1-1.5	1.25	0.148	0.011	0.023	0.002			2.6	0.7		
PAP-1.5-2	1.75	0.137	0.006	0.037	0.003	0.07	0.02	1.8	0.8	0.035	0.013
PAP-2-2.5	2.25	0.155	0.008	0.023	0.003			2.3	0.3		
PAP-2.5-3	2.75	0.141	0.013	0.010	0.004	0.6	0.2	7	3		
PAP-3.5-4	3.75	0.132	0.008	0.011	0.002	0.60	0.15	4.6	0.8	0.13	0.03
PAP-4-5	4.25	0.136	0.009	0.014	0.002	0.38	0.09	3.4	0.6	0.11	0.03
PAP-5-6	5.5	0.173	0.012	0.0026	0.0011	1.1	0.6	26	21	0.04	0.02
PAP-6-7	6.5	0.19	0.02	0.005	0.014			30	88		
PAP-7-8	7.5	0.17	0.02								
PAP-8-9	8.5	0.15	0.03								
PAP-9-10	9	0.18	0.04	0.036	0.027			15	17		
PAP-10-10.5	10.25	0.15	0.03								

Table 5
^{236}U, ^{129}I, $^{239+240}Pu$ and ^{137}Cs inventories calculated in the sediment core from PAP site. There have been included results from published inventories from sea-bed sediments, continental sediments and in the seawater column (Assinder et al., 1993; Bressac et al., 2017; Casacuberta et al., 2014; Garcia-Orellana et al., 2009; Gascó et al., 2006; Gomez-Guzman et al., 2013; Sakaguchi et al., 2012).

Inventories						
	^{236}U (at m^{-2})	$^{239+240}Pu$ (Bq m^{-2})	^{129}I (at m^{-2})	^{137}Cs (Bq m^{-2})	$^{236}U/^{239}Pu$ (at at^{-1})	$^{137}Cs/^{236}U$ (Bq at^{-1})
PAP site sediment	1,04E+12	4,51E+01	2,62E+12	83,08	0.0357	7,98E-11
Marine Sediment	1,50E+11	3,06E+00	1,30E+13	74,1	0.022	2,45E-10
Continental sediment	1,30E+13	5,00E+01	1,20E+14	2600	0.23	
Seawater column	1,50E+13	4,87E+01	3,40E+14	1652		1,21E-10

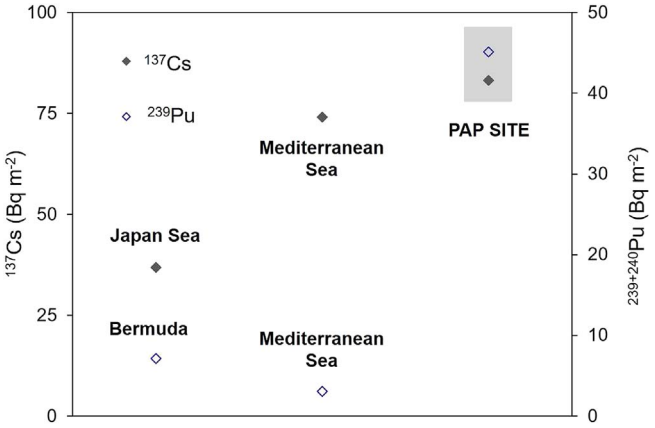

Fig. 5. Inventories of ^{137}Cs (mBq g^{-1}) and $^{239-240}Pu$ (mBq g^{-1}) in sea-bed sediment cores collected in different locations: Bermuda site (Buesseler and Sholkovitz, 1987), Japan Sea (Sakaguchi et al., 2012) and Mediterranean Sea (Garcia-Orellana et al., 2009) and PAP site (this paper).

between the ratios in sediments affected by NFRPs, 7–3.2 10^{-10} Bq at^{-1}, and in estuarine and deep-sea marine sediments associated to fallout, below $1{\cdot}10^{-11}$ Bq at^{-1}, at the South-West Spain and the Mediterranean Sea. Note that in the Northern Hemisphere, on one hand there is an additional input for ^{129}I associated to the gaseous emissions from the NFRPs that is preferential in certain areas according to the direction of the winds (Reithmeier et al., 2007). On the other hand, some areas in Europe. e.g. Mediterranean Sea, are significantly affected by ^{137}Cs deposition of the atmospheric releases from the Chernobyl

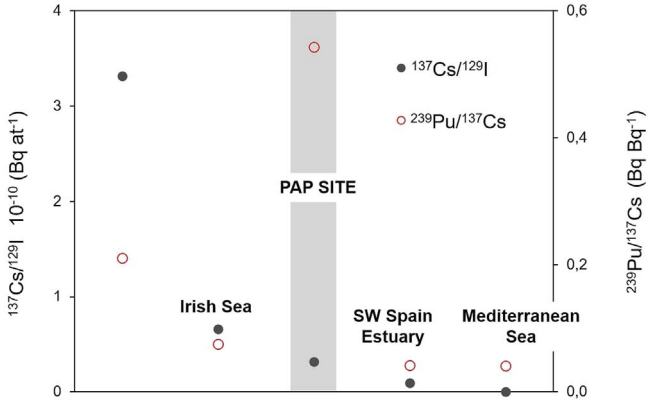

Fig. 6. Ratios $^{137}Cs/^{129}I$ (mBq at^{-1}) and $^{239-240}Pu/^{137}Cs$ (Bq Bq^{-1}) in sea-bed sediment cores collected in different locations: the first two columns correspond to the Irish Sea (Assinder et al., 1993), third column is the PAP site (this paper and finally respectively Estuary in South West Spain (Gascó et al., 2006) and Mediterranean Sea (Garcia-Orellana et al., 2009)).

accident (San Miguel et al., 2004) and finally, since the half-life of ^{137}Cs is 30 yr, lower values than the ones measured 10 years ago would be expected in the present. $^{137}Cs/^{129}I$ at the PAP site, $3.2{\cdot}10^{-11}$ Bq at^{-1}, is within the expected values for an atmospheric deposition from fallout and gaseous emissions from the NFRPs; the slightly higher values measured at PAP site than the ones at SW Spain and the Mediterranean Sea, probably corresponds to a lower contribution of the ^{129}I gaseous emissions from NFRPs in the area.

$^{239+240}Pu/^{137}Cs$ at PAP site is 0.54 Bq at^{-1} and strongly diverge from the values at the Irish Sea, 0.2–0.08 Bq at^{-1} and the fallout values, below 0.4 Bq at^{-1}. This is due to the high contribution of $^{239+240}Pu$, to the inventory ratio. The existence of an additional $^{239+240}Pu$ source is hypothesized.

We conclude that the inventories and the isotopic ratios at this PAP site core correspond to a marine sediment sample with a main contribution of fallout. The contribution of an additional source, unrelated to NFRP should be further explored.

3.3. Radioactive sources

In the previous sections some signs of an additional radioactive source were observed and should be further investigated. If we assume a similar contribution of global fallout at the PAP site (49°N) and at the Japan Sea (39°N), similar anthropogenic radionuclides inventories in the corresponding sediment cores would be expected, taking into account that both locations can be considered open-ocean sites, where the atmosphere constitutes the only significant source of natural lithogenic and anthropogenic material. However, ^{236}U inventory at the PAP site is

almost an order of magnitude higher, despite the depth differences (i.e. 4000 m and 2800 m depth, respectively) (Table 5). The origin of this increase is not associated to higher particle fluxes at PAP site that would scavenge more ^{236}U in the North Atlantic Ocean than at the Japan Sea. Because carbon export flux from surface to 2000m is similar in both locations 2 gC m^{-2} y^{-1} (Henson et al., 2012; Honjo et al., 2008) and then a similar scavenging of ^{236}U at the PAP site and Japan Sea should be assumed. The influence of Saharian dust in the radionuclides input and scavenge at the PAP site should be further investigated, but differences of one order of magnitude for ^{236}U deposition are not expected (Pham et al., 2017).

There is a small fraction of the discharges from the NFRPs that do not reach the Norwegian Coastal Current and, on the contrary, is dispersed to the south-west of the North Atlantic Ocean. This is suggested by a model that predicts the fate of ^{129}I and ^{137}Cs releases from the NFRP in the North Atlantic Sea (Periáñez et al., 2016; Villa-Alfageme et al., 2015). However, the higher inventories of $^{239+240}$Pu and ^{236}U in the sediment core cannot be associated to this fraction. In the case of particle reactive plutonium, it will be scavenged from the water before arriving to the PAP site. In the case of conservative ^{236}U, according to Villa-Alfageme et al. (2015), the contribution of NFRP to the, also conservative, ^{129}I concentrations at the PAP site is lower to the contribution of fallout. If a similar trend were maintained for ^{236}U, this fraction of the NFRP releases could not account for the ^{236}U increase of almost one order of magnitude in the sediment. Similarly, using the same dispersion model (Periáñez et al., 2016), they estimated negligible concentrations of ^{137}Cs in the sediments at the PAP site area.

We believe that the higher values of ^{236}Pu and ^{236}U might be associated to leakages from the dumped nuclear wastes located in several locations of the Northeast Atlantic, close to the coasts of Galicia and Ireland (IAEA, 2015). In a routinely survey carried out in 1992 to these wasted, elevated concentrations of several radionuclides, e.g. ^{14}C, ^{137}Cs, ^{241}Am and $^{239+240}$Pu, indicating leakages from the packages (IAEA, 2015). These leakages are increasing preferentially the concentration of ^{236}U at the surface of the PAP site in contrast to the less mobile plutonium. Periáñez et al. (2016) showed in their model that the ^{137}Cs contribution from these leakages to the sea-bed should not have radioecological implications; though it could be the cause of the significant increase in the radionuclide concentrations of ^{236}U and $^{239+240}$Pu and, to a lesser extent, ^{137}Cs. The lack of data from other marine sediments in the area and the lack of data regarding the radiological composition and the age – and this is of key importance in the case of radionuclides of short half-lives such as ^{137}Cs - of the dumped nuclear wastes prevents us to reach definitive conclusions and further studies are suggested.

4. Conclusions

Most of the anthropogenic radioactivity due to fall-out and particles deposition should be located in the very first centimetres of the sediment, however ^{137}Cs, ^{236}U and ^{129}I and even the most particle reactive radionuclides ^{210}Pb and $^{239+240}$Pu are mobile in this core that presents two maximums in depth. This indicates that the sediment has been possibly perturbed due to bioturbation.

In the sediment analysed ^{236}U behaviour differs from the one of conservative and mobile ^{129}I and ^{137}Cs. When the results for ^{236}U are zoomed below the surface and mobile and a refractory responses are compared we find out that in this sediment the behaviour of uranium is more similar to a particle reactive radionuclide. This points out to a possible reduction, due to the anoxic conditions of the sediment, of ^{236}U from mobile U(VI) to more refractory U(IV).

The higher inventories of ^{236}U, $^{239+240}$Pu and to a lesser extent ^{137}Cs, measured at the PAP site in comparison to other marine sediments from the Northern Hemisphere are not associated to a higher particle export at the PAP site and the contribution from Sellafield and La Hague Nuclear Reprocessing Plants is also discarded. Sediments might be influenced by the potential leakages from the dumped nuclear wastes located nearby in several locations of the Northeast Atlantic.

Acknowledgment

We would like to thank the captain and crew of the RRS Discovery and the D341 scientific team. This work was partly supported by Spanish MINECO research project No. FIS2015-69673-P.

References

Ahmad, I., Kondev, F.G., Greene, J.P., Kellett, M.A., Nichols, A.L., 2007. Measurement of the 240Pu half-life. Nuclear instruments and methods in physics research section A. Accelerators, Spectrometers, Detect. Assoc. Equip. 579, 458–460.
Assinder, D., Yamamoto, M., Kim, C., Seki, R., Takaku, Y., Yamauchi, Y., Igarashi, S., Komura, K., Ueno, K., 1993. Radioisotopes of thirteen elements in intertidal coastal and estuarine sediments in the Irish Sea. J. Radioanal. Nucl. Ch 170, 333–346.
Bett, B.J., Malzone, M.G., Narayanaswamy, B.E., Wigham, B.D., 2001. Temporal variability in phytodetritus and megabenthic activity at the seabed in the deep Northeast Atlantic. Prog. Oceanogr. 50, 349–368.
Billett, D., Bett, B., Reid, W., Boorman, B., Priede, I., 2010. Long-term change in the abyssal NE atlantic: the 'Amperima Event'revisited. Deep sea research Part II. Top. Stud. Oceanogr. 57, 1406–1417.
Billett, D., Bett, B., Rice, A., Thurston, M., Galéron, J., Sibuet, M., Wolff, G., 2001. Long-term change in the megabenthos of the porcupine Abyssal plain (NE atlantic). Prog. Oceanogr. 50, 325–348.
Bressac, M., Levy, I., Chamizo, E., La Rosa, J., Povinec, P., Gastaud, J., Oregioni, B., 2017. Temporal evolution of 137 Cs, 237 Np, and 239+ 240 Pu and estimated vertical 239+ 240 Pu export in the northwestern Mediterranean Sea. Sci. Total Environ. 595, 178–190.
Buesseler, K.O., Sholkovitz, E.R., 1987. The geochemistry of fallout plutonium in the North Atlantic: II. 240Pu239Pu ratios and their significance. Geochim. Cosmochim. Ac 51, 2623–2637.
Calvo, E.C., Santos, F.J., López-Gutiérrez, J.M., Padilla, S., Garcia-Leon, M., Heinemeier, J., Schnabel, C., Scognamiglio, G., 2015. Status report of the 1MV AMS facility at the Centro Nacional de Aceleradores. Nucl. Instrum. Methods Phys. Res. Sect. B Beam Interact. Mater. Atoms 361, 13–19.
Carvalho, F.P., Oliveira, J.M., Soares, A.M.M., 2011. Sediment accumulation and bioturbation rates in the deep Northeast Atlantic determined by radiometric techniques. ICES J. Mar. Sci. 68, 427–435.
Casacuberta, N., Christl, M., Lachner, J., Rutgers van der Loeff, M., Masqué, P., Synal, H.-A., 2014. A first transect of 236U in the North Atlantic Ocean. Geochim. Cosmochim. Ac 133, 34–46.
Casacuberta, N., Masqué, P., Henderson, G., Rutgers van-der-Loeff, M., Bauch, D., Vockenhuber, C., Daraoui, A., Walther, C., Synal, H.A., Christl, M., 2016. First 236U data from the Arctic Ocean and use of 236U/238U and 129I/236U as a new dual tracer. Earth Planet Sc Lett. 440, 127–134.
Castrillejo, M., Casacuberta, N., Christl, M., Garcia-Orellana, J., Vockenhuber, C., Synal, H.A., Masqué, P., 2017. Anthropogenic 236U and 129I in the Mediterranean Sea: first comprehensive distribution and constrain of their sources. Sci. Total Environ. 593–594, 745–759.
Cumberland, S.A., Douglas, G., Grice, K., Moreau, J.W., 2016. Uranium mobility in organic matter-rich sediments: a review of geological and geochemical processes. Earth-Science Rev. 159, 160–185.
Chamizo, E., Jiménez-Ramos, M.C., Wacker, L., Vioque, I., Calleja, A., García-León, M., García-Tenorio, R., 2008. Isolation of Pu-isotopes from environmental samples using ion chromatography for accelerator mass spectrometry and alpha spectrometry. Anal. Chim. Acta 606, 239–245.
Chamizo, E., López-Lora, M., Villa, M., Casacuberta, N., López-Gutiérrez, J.M., Pham, M.K., 2015. Analysis of 236U and plutonium isotopes, 239,240Pu, on the 1 MV AMS system at the Centro Nacional de Aceleradores, as a potential tool in oceanography. Nucl. Instrum. Methods Phys. Res. Sect. B Beam Interact. Mater. Atoms 361, 535–540.
Christl, M., Casacuberta, N., Vockenhuber, C., Elsässer, C., Bailly du Bois, P., Herrmann, J., Synal, H.A., 2015. Reconstruction of the 236U input function for the Northeast Atlantic Ocean: implications for 129I/236U and 236U/238U-based tracer ages. J. Geophys. Res. Oceans 120, 7282–7299.
Christl, M., Lachner, J., Vockenhuber, C., Goroncy, I., Herrmann, J., Synal, H.-A., 2013. First data of Uranium-236 in the North sea. Nucl. Instrum. Methods Phys. Res. Sect. B Beam Interact. Mater. Atoms 294, 530–536.
Christl, M., Lachner, J., Vockenhuber, C., Lechtenfeld, O., Stimac, I., van der Loeff, M.R., Synal, H.A., 2012. A depth profile of uranium-236 in the Atlantic Ocean. Geochim. Cosmochim. Ac 77, 98–107.
Eigl, R., Steier, P., Sakata, K., Sakaguchi, A., 2017. Vertical distribution of 236U in the North Pacific Ocean. J. Environ. Radioact. 169–170, 70–78.
Flynn, K.F., Jaffey, A.H., Bentley, W.C., Essling, A.M., 1972. Precision measurement of half-life and specific activity of 236U. J. Inorg. Nucl. Chem. 34, 1121–1129.
Garcia-Orellana, J., Pates, J.M., Masqué, P., Bruach, J., Sanchez-Cabeza, J., 2009. Distribution of artificial radionuclides in deep sediments of the Mediterranean Sea. Sci. Total Environ. 407, 887–898.
Gascó, C., Antón, M.P., Pozuelo, M., Clemente, L., Rodríguez, A., Yanez, C., González, A., Meral, J., 2006. Distribution and inventories of fallout radionuclides (239+ 240 Pu,

137 Cs) and 210 Pb to study the filling velocity of salt marshes in Doñana National Park (Spain). J. Environ. Radioact. 89, 159–171.
Gómez-Guzmán, J., López-Gutiérrez, J., Pinto-Gómez, A., Holm, E., 2012. 129 I measurements on the 1MV AMS facility at the Centro Nacional de Aceleradores (CNA, Spain). Appl. Radiat. Isot. 70, 263–268.
Gomez-Guzman, J.M., Villa-Alfageme, M., Le Moigne, F., Lopez-Gutierrez, J.M., Garcia-Leon, M., 2013. AMS measurements of I-129 in seawater around Iceland and the Irminger Sea. Nucl. Instrum. Meth B 294, 547–551.
Hajdas, I., Bonani, G., Thut, J., Leone, G., Pfenninger, R., Maden, C., 2004. A report on sample preparation at the ETH/PSI AMS facility in Zurich. Nuclear instruments and methods in physics research section B. Beam Interact. Mater. Atoms 223, 267–271.
Henson, S.A., Sanders, R., Madsen, E., 2012. Global patterns in efficiency of particulate organic carbon export and transfer to the deep ocean. Glob. Biogeochem. Cy 26.
Honjo, S., Manganini, S., Krishfield, R.A., Francois, R., 2008. Particulate organic carbon fluxes to the ocean interior and factors controlling the biological pump: a synthesis of global sediment trap programs since 1983. Prog. Oceanogr. 76, 217–285.
Hurtado, S., Garcia-Leon, M., Garcia-Tenorio, R., 2006. Optimized background reduction in low-level gamma-ray spectrometry at a surface laboratory. Appl. Radiat. Isot. 64, 1006–1012.
IAEA, 2015. Inventory of Radioactive Material Resulting from Historical Dumping Accidents and Losses at Sea. IAEA, Vienna.
Jiménez-Ramos, M., Hurtado, S., Chamizo, E., García-Tenorio, R., León-Vintró, L., Mitchell, P., 2010. 239Pu, 240Pu, and 241Am determination in hot particles by low level gamma-spectrometry. Environ. Sci. Technol. 44, 4247–4252.
Juget, F., Nedjadi, Y., Buchillier, T., Bochud, F., Bailat, C., 2016. Determination of 137Cs half-life with an ionization chamber. Appl. Radiat. Isot. 118, 215–220.
Kalogeropoulou, V., Bett, B., Gooday, A., Lampadariou, N., Arbizu, P.M., Vanreusel, A., 2010. Temporal changes (1989–1999) in deep-sea metazoan meiofaunal assemblages on the Porcupine Abyssal Plain, NE Atlantic. Deep Sea Res. Part II Top. Stud. Oceanogr. 57, 1383–1395.
Kelley, J., Bond, L., Beasley, T., 1999. Global distribution of Pu isotopes and 237 Np. Sci. Total Environ. 237, 483–500.
Ketterer, M.E., Hafer, K.M., Link, C.L., Royden, C.S., Hartsock, W., 2003. Anthropogenic U-236 at Rocky Flats, Ashtabula river harbor, and Mersey estuary: three case studies by sector inductively coupled plasma mass spectrometry. J. Environ. Radioact. 67, 191–206.
Laissaoui, A., Mas, J.L., Hurtado, S., Ziad, N., Villa-Alfageme, M., Benmansour, M., 2013. Radionuclide activities and metal concentrations in sediments of the Sebou Estuary, NW Morocco, following a flooding event. Environ. Monit. Assess. 185, 5019–5029.
Le Moigne, F.A.C., Villa, M., Sanders, R.J., Marsay, C., Henson, S.R., García-Tenorio, R., 2013. Export of organic carbon and biominerals derived from 234Th and 210Po at the Porcupine Abyssal Plain. Deep-Sea Res. Pt I 72, 88–101.
Lépy, M.-C., Altzitzoglou, T., Anagnostakis, M., Capogni, M., Ceccatelli, A., De Felice, P., Djurasevic, M., Dryak, P., Fazio, A., Ferreux, L., 2012. Intercomparison of methods for coincidence summing corrections in gamma-ray spectrometry—part II (volume sources). Appl. Radiat. Isot. 70, 2112–2118.
Maher, K., Bargar, J.R., Brown Jr., G.E., 2012. Environmental speciation of actinides. Inorg. Chem. 52, 3510–3532.
Mann, W., 1983. An international reference material for radiocarbon dating. Radiocarbon 25, 519–527.
Mantero, J., Gázquez, M., Hurtado, S., Bolívar, J., García-Tenorio, R., 2015. Application of gamma-ray spectrometry in a NORM industry for its radiometrical characterization. Radiat. Phys. Chem. 116, 78–81.
Marsden, O.J., Livens, F.R., Day, J.P., Fifield, L.K., Goodall, P.S., 2001. Determination of U-236 in sediment samples by accelerator mass spectrometry. Analyst 126, 633–636.
Morris, K., Raiswell, R., 2002. Chapter 4 Biogeochemical cycles and remobilisation of the actinide elements. Radioact. Environ. 101–141.
Mougeot, X., 2017. Improved calculations of electron capture transitions for decay data and radionuclide metrology. Appl. Radiat. Isot (in press).
Nomura, T., Sakaguchi, A., Steier, P., Eigl, R., Yamakawa, A., Watanabe, T., Sasaki, K., Watanabe, T., Golser, R., Takahashi, Y., Yamano, H., 2017. Reconstruction of the temporal distribution of 236U/238U in the Northwest Pacific Ocean using a coral core sample from the Kuroshio Current area. Mar. Chem. 190, 28–34.
Owens, S.A., Buesseler, K.O., Sims, K.W.W., 2011. Re-evaluating the 238U-salinity relationship in seawater: implications for the 238U–234Th disequilibrium method. Mar. Chem. 127, 31–39.
Periáñez, R., Suh, K.-S., Min, B.-I., 2016. The behaviour of 137Cs in the North Atlantic Ocean assessed from numerical modelling: releases from nuclear fuel reprocessing factories, redissolution from contaminated sediments and leakage from dumped nuclear wastes. Mar. Pollut. Bull. 113, 343–361.
Pettitt, P.B., Davies, W., Gamble, C.S., Richards, M.B., 2003. Palaeolithic radiocarbon chronology: quantifying our confidence beyond two half-lives. J. Archaeol. Sci. 30, 1685–1693.
Pham, M.K., Chamizo, E., Mas Balbuena, J.L., Miquel, J.-C., Martín, J., Osvath, I., Povinec, P.P., 2017. Impact of Saharan dust events on radionuclide levels in Monaco air and in the water column of the northwest Mediterranean Sea. J Environ Radioactiv 166. Part 1, 2–9.
Prindle, A., Evans, J., Dupzyk, R., Nagle, R., Newbury, R., 1978. The half life of 239Pu. Int. J. Appl. Radiat. Isot. 29, 517–524.
Raisbeck, G.M., Yiou, F., 1999. 129I in the oceans: origins and applications. Sci. Total Environ. 237, 31–41.
Reithmeier, H., Lazarev, V., Rühm, W., Nolte, E., 2007. 129 I measurements in lake water for an estimate of regional 129 I depositions. Sci. Total Environ. 376, 285–293.
Richter, S., Alonso, A., Aregbe, Y., Eykens, R., Jacobsson, U., Kehoe, F., Kuehn, H., Verbruggen, A., Wellum, R., 2010. Certification of a new series of gravimetrically prepared synthetic reference materials for n(U-236)/n(U-238) isotope ratio measurements. Nucl. Instrum. Meth B 268, 956–959.
Rozanski, K., Stichler, W., Gonfiantini, R., Scott, E., Beukens, R., Kromer, B., Van Der Plicht, J., 1992. The IAEA 14 C intercomparison exercise 1990. Radiocarbon 34, 506–519.
Sakaguchi, A., Kadokura, A., Steier, P., Takahashi, Y., Shizuma, K., Hoshi, M., Nakakuki, T., Yamamoto, M., 2012. Uranium-236 as a new oceanic tracer: a first depth profile in the Japan Sea and comparison with caesium-137. Earth Planet Sc Lett. 333, 165–170.
Sakaguchi, A., Kawai, K., Steier, P., Quinto, F., Mino, K., Tomita, J., Hoshi, M., Whitehead, N., Yamamoto, M., 2009. First results on (236)U levels in global fallout. Sci. Total Environ. 407, 4238–4242.
San Miguel, E.G., Bolivar, J.P., García-Tenorio, R., 2004. Vertical distribution of Th-isotope ratios, 210Pb, 226Ra and 137Cs in sediment cores from an estuary affected by anthropogenic releases. Sci. Total Environ. 318, 143–157.
San Miguel, E.G., Perez-Moreno, J.P., Bolivar, J.P., Garcia-Tenorio, R., 2003. Validation of isotope signatures in sediments affected by anthropogenic inputs from uranium series radionuclides. Environ. Pollut. 123, 125–130.
Santos Arévalo, F.-J., Gómez Martínez, I., Agulló García, L., 2015. 14C SIRI samples at CNA: measurements at 200 kV and 1000 kV. Nucl. Instrum. Methods Phys. Res. Sect. B Beam Interact. Mater. Atoms 361, 322–326.
Steier, P., Bichler, M., Fifield, L.K., Golser, R., Kutschera, W., Priller, A., Quinto, F., Richter, S., Srncikf, M., Terrasi, P., Wacker, L., Wallner, A., Wallner, G., Wilcken, K.M., Wild, E.M., 2008. Natural and anthropogenic (236)U in environmental samples. Nucl. Instrum. Meth B 266, 2246–2250.
Stordal, M., Johnson, J., Guinasso, N., Schink, D., 1985. Quantitative evaluation of bioturbation rates in deep ocean sediments. II. Comparison of rates determined by 210Pb and 239,240 Pu. Mar. Chem. 17, 99–114.
Stuiver, M., Polach, H.A., 1977. Discussion reporting of 14 C data. Radiocarbon 19, 355–363.
Szidat, S., Schmidt, A., Handl, J., Jakob, D., Botsch, W., Michel, R., Synal, H.-A., Schnabel, C., Suter, M., Lopez-Gutierrez, J., 2000. Iodine-129: sample preparation, quality control and analyses of pre-nuclear materials and of natural waters from Lower Saxony, Germany. Nuclear Instruments and Methods in Physics Research Section B. Beam Interact. Mater. Atoms 172, 699–710.
Vidmar, T., Aubineau-Laniece, I., Anagnostakis, M., Arnold, D., Brettner-Messler, R., Budjas, D., Capogni, M., Dias, M., De Geer, L., Fazio, A., 2008. An intercomparison of Monte Carlo codes used in gamma-ray spectrometry. Appl. Radiat. Isot. 66, 764–768.
Villa-Alfageme, M., de Soto, F., Le Moigne, F.A.C., Giering, S., Salvador, M., Sanders, R., 2014. Observations and modeling of slow sinking particles in the Twilight zone. Glob. Biogeochem. Cy 28, 1327–1342.
Villa-Alfageme, M., López-Gutiérrez, J.M., Kyung-Suk, S., Byung-Il, M., Periañez, R., 2015. The behaviour of 129I released from nuclear fuel reprocessing factories in the North Atlantic Ocean and transport to the Arctic assessed from numerical modelling. Mar. Pollut. Bull. 90, 15–24.
Villa, M., Manjón, G., García-León, M., 2003. Study of colour quenching effects in the calibration of liquid scintillation counters: the case of 210Pb. Nuclear Instruments and Methods in Physics Research Section A. Accel. Spectrom. Detect. Assoc. Equip. 496, 413–424.
Villa, M., Moreno, H.P., Manjón, G., 2005. Determination of 226Ra and 224Ra in sediments samples by liquid scintillation counting. Radiat. Meas. 39, 543–550.
Villa, M., Mosqueda, F., Hurtado, S., Mantero, J., Manjon, G., Perianez, R., Vaca, F., Garcia-Tenorio, R., 2009. Contamination and restoration of an estuary affected by phosphogypsum releases. Sci. Total Environ. 408, 69–77.
Wacker, L., Bonani, G., Friedrich, M., Hajdas, I., Kromer, B., Němec, M., Ruff, M., Suter, M., Synal, H., Vockenhuber, C., 2010a. MICADAS: routine and high-precision radiocarbon dating. Radiocarbon 52, 252–262.
Wacker, L., Christl, M., Synal, H.-A., 2010b. Bats: a new tool for AMS data reduction. Nucl. Instrum. Methods Phys. Res. Sect. B Beam Interact. Mater. Atoms 268, 976–979.
Wacker, L., Němec, M., Bourquin, J., 2010c. A revolutionary graphitisation system: fully automated, compact and simple. Nuclear Instruments and Methods in Physics Research Section B. Beam Interact. Mater. Atoms 268, 931–934.
Wendel, C.C., Oughton, D.H., Lind, O.C., Skipperud, L., Fifield, L.K., Isaksson, E., Tims, S.G., Salbu, B., 2013. Chronology of Pu isotopes and U-236 in an Arctic ice core. Sci. Total Environ. 461, 734–741.
Winkler, S.R., Steier, P., Carilli, J., 2012. Bomb fall-out U-236 as a global oceanic tracer using an annually resolved coral core. Earth Planet Sc Lett. 359, 124–130.